Spatial scene representation and navigation in a mobile robot using RGB-D camera

Marek Jaszuk, University of Information Technology and Management, Rzeszów, Poland
Wojciech Pałka, Academic High School, Rzeszów, Poland
Michał Furgał, University of Information Technology and Management, Rzeszów, Poland
Dawid Darłak, Academic High School, Rzeszów, Poland
Janusz A. Starzyk, School of Electrical Engineering and Computer Science Ohio University, Athens, USA, and University of Information Technology and Management, Rzeszów, Poland

Abstract

The paper presents an algorithm for creating 3D scene representation to be used in a mobile robot. The operation of the algorithm is based on data collected with an RGB-D camera. The RGB scene view is further processed with instance segmentation algorithm based on convolutional neural networks to obtain binary masks of the recognized objects. The masks are matched to the depth view of the scene, which gives point clouds reflecting 3D shape of objects. Then the point clouds are averaged to reduce all objects into single points. In this way we obtain minimalistic representation of a scene, which is easy for storing and processing even in case of very large and complex scenes. This scene representation is aimed to support a mobile robot in recognizing scenes, and finding locations. The experiments were based on the Parallax Arlo robotic platform, and the Microsoft Kinect for Azure camera.

1 Introduction

The problem of 3D scene mapping has been addressed by many researchers. This task is of particular importance for autonomous robots that have to track in real-time their location and create an internal representation of the scene, which is known as simultaneous location and mapping (SLAM)[1]. The approach in this area is the visual SLAM (vSLAM) [2], which is based purely on image analysis. It gained its popularity in wide range of applications due to availability of cheap cameras in various kinds of devices. While vSLAM allows for collecting large amount of data, it is not very precise. To get more precise scene reproduction it is better to use distance sensors such as LIDAR scanners or RGB-D cameras. 3D map of a scene, can be created in this case by combining the video data, and the spatial data. While using LIDAR scanners is still an expensive solution, the RGB-D cameras are relatively cheap. The most notable device from this category is Microsoft Kinect. When combined with KinectFusion software package it allows for reconstructing surface model of the scene even in real-time [3]. The device can also be mounted on a mobile robot to support the scene perception [4]. The interest in using the Kinect camera, has revived recently due to introducing the new generation of the device named Kinect for Azure.

In many applications of autonomous robots, the geometrical reconstruction of the scene is not sufficient, because the robot needs deeper understanding of the scene. This is especially important, when a robot needs to find objects of different types to perform some operations on them. The task of scene reconstruction accompanied by recognizing types of scene elements is known as semantic SLAM, see e.g. [5], [6], [7].

Recognition of semantic categories of scene elements is possible due analysis of the video data using deep convolutional neural networks [8]. For the robot it is important to recognize the category of the object, as well as to find its location. In the simplest case location is indicated by identifying the rectangle surrounding the recognized object like in the Faster R-CNN algorithm [9]. The rectangle, however, is very imprecise approximation, because it does not reflect the shape of the objects. To obtain the precise shape information, it is necessary to create the binary masks matching the pixels belonging to each object, which is known as instance segmentation. One of the first examples of such algorithms is the Mask R-CNN [10], which is an extension of Faster R-CNN.

For real-time systems, besides precision of results, we also have to take into account the speed of the computations. Using GPU acceleration is currently a standard approach. This still, however, not always provides sufficient speed. The mentioned Faster R-CNN algorithm allows for processing of about 7 frames per second (FPS) on a GPU. This is quite fast, but for real-time systems, larger frame rate is expected. The situation has been greatly improved by introduction of the fast single-stage algorithms of object detection, like YOLO [11], which allow for processing at the speed rate exceeding 40 FPS. The instance segmentation is, however, a more computationally intensive task. While most research is focused on improving precision of segmentation, not much work was devoted to speed of computations. One of the first approaches to treat this problem is the YOLACT algorithm [12]. This is a one-stage instance

segmentation tool, which allows for achieving 30+ FPS rate on a GPU, which is sufficient for real-time robot operation. Despite precision achieved by YOLACT is lower than the one achieved by the current state-of-the-art instance segmentation algorithms, we decided to use this tool due to its advantageous speed.
The last thing that we have to discuss is the scene representation. There are two most widely applied methods of 3D world representation: surface models and voxel models. Both of them are applied in robotics [13][14] for building scene representation. Both kinds of scene representation have their advantages and disadvantages. The main disadvantage of both of them is that they collect massive amounts of data, which are hard to handle. While the precise scene reproduction is of key importance in many applications, our goal focused on memorizing only the key objects within the scene. If the memorized environment is large and contains a rich variety of scenes, it is hard to recognize the scene of interest, and locate the robot within the world, unless an external location system, like GPS, is available. The speed of memory processing is also critical, if the robot needs to compare the perceived scene with the memory during its normal operation, i.e. in real time. The scene representation presented in this work is addressed to solve such problems.
In our approach the scene representation complexity is reduced maximally by memorizing objects as points. This might seem simplistic, but allows for storing the minimum of necessary information about the scene. The other, less important details might be used only temporarily when the robot perceives the scene, e.g. for collision avoidance, but they are not stored permanently in the memory.
The paper is organized as follows. In Section 2 we describe building local scene representation. In particular, we describe the experimental setup and the method of matching visually recognized objects to the depth data, and identifying point location of the objects in the local view of the robot. In Section 3 we describe the algorithm of transforming the local coordinates of objects to the scene model and present test results. Section 4 presents the conclusions.

2 Building local scene representation

In this section we analyze the mechanism of building internal scene representation by a mobile robot exploring a 3D scene.

2.1 Previous work

We already presented the basic mechanism for creating the discussed kind of scene representation, but that work was related to an agent exploring a virtual world created using a game engine [15]. This simplified the problem, because the mobile agent could use the data delivered by the game engine used to create a digital world. When dealing with the real world data registered during mobile robot operation, such simplification is not possible, and we have to overcome all the difficulties coming from imperfect object recognition, incompleteness of information, and different kinds of noises. We also developed a method for comparing scenes, which allows for deciding if the scene was already memorized by the robot, or not [15]. The method is based on the distance matrix created for the scene, which is then compared to the memorized scene, and gives the similarity factor between both the scenes.

2.2 The experimental set

The robot that we use in our experiments is the Parallax Arlo mobile platform, which allows for easy mounting of additional equipment (**Figure 1**). On the top of the platform we mounted the RGB-D camera, which in our case is the Microsoft Kinect for Azure. This is our only sensor delivering information about the scene. Single shot taken by the robot from a particular location gives only information about the positions of scene elements which are in the range of the depth camera measurements. In most of the devices available on the market, this range does not exceed several meters.

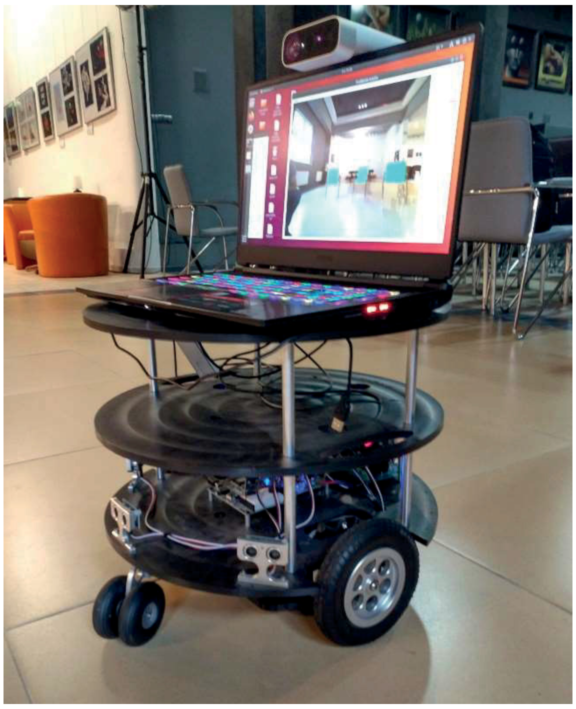
Figure 1 The Arlo mobile robot platform with the Kinect for Azure sensor used in experiments

To export the most computationally intensive parts of data processing, we extended our experimental set by a computational server equipped with GPU cards. Thus, the main robot data processing system is located on the server. A laptop placed on the platform receives the depth and RGB scene view from the sensor, and sends them to the server through local Wi-Fi connection. After the data have been processed on the server and the robot steering system makes the decision about further robot operation, the appropriate signals are sent back to the laptop. Then the laptop sends the commands to the robot microcontroller, which transforms them into rotation of the robot wheels. The speed of data transmission in contemporary computer networks is not a significant limitation, thus the robot can operate without notable delays. The experimental advantage of moving computations to the server, is that we can preview in real time the internal states of the robot during its operation.

2.3 Locating objects in 3D space

On the server the RGB scene view undergoes processing using tools based on convolutional neural networks. This allows for recognition and location of a set of objects within the robot's field of view (**Figure 2**). The recognition and location is, however, not sufficient, because our approach assumes, that the shape of the object must be identified so that it will be easier to manipulate. There is a number of tools that can be used for this purpose, and we analyzed the available choices. Our initial choice was to use the Mask R-CNN [10]. To train the model we created our own dataset representing the objects that can be found inside our university building, like different kinds of furniture.

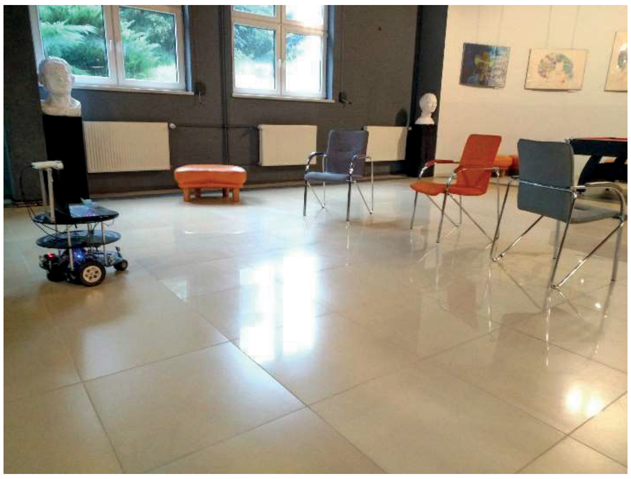

Figure 2 The robot facing the scene

The Mask R-CNN itself allows for processing speed of about 5 FPS. But we have to take into account, that image masking, although the most computationally intensive element of the processing sequence, is not the only operation performed by the main robot steering system. Thus, the real speed of the system operation was a bit lower - approximately 3 FPS.

Assuming that the robot is not going to move very quickly, this speed of operation could be accepted. The experiments showed, however, that the results generated by the Mask R-CNN are not stable. The instability is revealed in the fact that in a sequence of images received from the robot, at least some objects are not always masked, despite that they are visible very well. For the robot perception, this means, that some objects appear and disappear. It is also possible, that the object changes its type between subsequent frames. This happens in case of high similarity between two categories. This kind of effects makes it quite hard to maintain a stable scene view. It is not possible to eliminate this effect by longer training or delivering more training data.

We tried also alternative tools, and all of them demonstrated this kind of instability. The only solution to the problem, that we could find, was to cumulate the results from a sequence of images, which would make the scene perception more stable. Such cumulation will cause, however, further slowing down of the sensory data processing. The improvement could be brought by, a faster masking algorithm, which still maintains stability of results, and quality of masks at least comparable to Mask R-CNN. It is not an easy task, because most of the available algorithms operate with speed not larger than a few FPS.

Our expectations were met by YOLACT [12]. The implementation of this algorithm allows for processing 30 FPS with high quality of masks. In this way, we obtain the binary masks of the objects (**Figure 3**). Within the illustrated scene three objects were recognized: one orange chair and 2 gray chairs (indicated by the text inside the surrounding rectangles). Although the algorithm is not stable, the higher processing speed of YOLACT allows for processing more frames per second. We introduced the confidence factor for each memorized object, which adds confidence point each time, the object is found in a given location, and subtracts a point when the object was not found where it was expected. If the confidence factor reaches 0, the object is no longer stored in the memory. This stabilizes the memory, despite instability in vision.

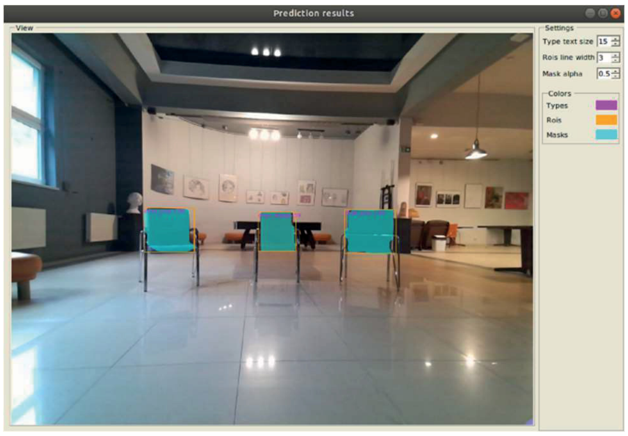

Prediction results
View
Settings
Type text size 15
Rois line width 3
Mask alpha 0.5
Colors
Types 🟪
Rois 🟧
Masks 🟦

Figure 3 The binary masks of objects obtained from YOLACT

Besides the contours of the recognized objects, we need to determine their location in 3D space using information from the depth camera. The raw depth view obtained from Kinect is shown in **Figure 4**. Each pixel in the image represents the distance from the camera to respective element of the scene. Such a spatial data representation is not convenient for further computations. Thus, we transform the depth data into a point cloud. The point cloud is equivalent of the depth image, but it represents not the distance from the camera, but the points in 3D coordinates with the origin in the camera location. The code that we implemented to do that is written using CUDA to accelerate the computation on a GPU. The point cloud obtained for the discussed scene view is presented in **Figure 5**. The figure indicates also the point locations of particular objects. To get them we match the binary masks from **Figure 3** to the point cloud. In this way we obtain a filtered point cloud (**Figure 6**). Then we average all the filtered points to obtain single point locations of individual objects within the local camera coordinates.

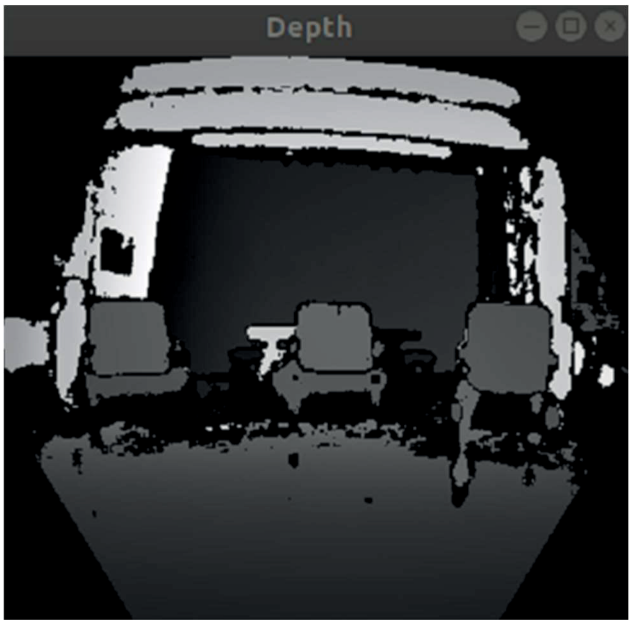

Figure 4 The depth view of the scene

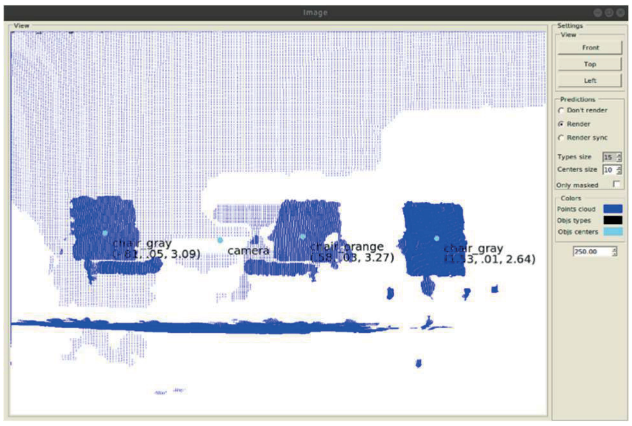

Figure 5 The frontal point cloud view

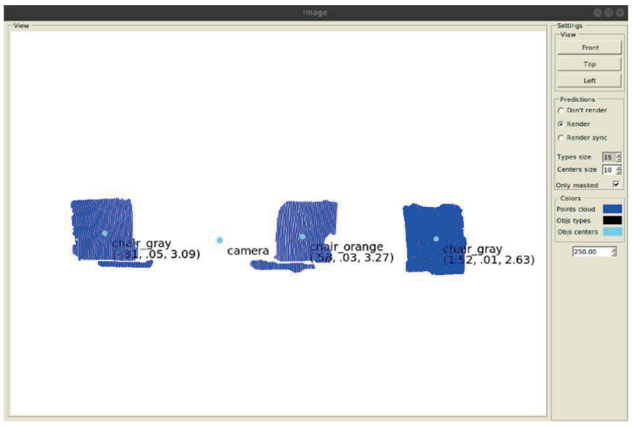

Figure 6 The filtered frontal point cloud view

We use the coordinate system typical for 3D graphics, where the z axis is pointing towards the scene, the y axis is pointing up, and the x axis is pointing to the right. The camera location is (0, 0, 0). The locations of objects in the camera coordinates are the basis for building the scene memory.

As one can see in **Figure 3**, the masks generated for the chairs do not cover their legs. This is not due to limited accuracy of the masking algorithm, but deliberate action. We prepared the training data in this way, to avoid including the chair legs. The reason for that is the depth data (**Figure 5**), where we can see that the legs of the chairs are mainly black. The black color means, that the location is undetermined, and in consequence, these elements are mostly invisible in the point cloud (**Figure 5**). Trying to include them would only increase fluctuations in the object locations. The reason is the metallic reflective material, which reveals the camera limitation.

The obvious limitation of determining point locations of objects in a scene is that we don't know the whole shape of the object when we see it only from a single robot position. The position of the same object, can be different, when it is seen from another perspective. The robot while exploring the scene registers new views all the time, and can discover new, previously invisible, parts of the already identified objects. Thus, the position of the object is not something fixed, but it must be updated along with the scene exploration. This would lead to instability of the robot memory, which is undesirable. Thus, we developed an efficient way of stabilizing locations of objects in the memory, which is discussed in the next section.

3 Scene representation

The scene view obtained from a single robot position is not suitable for memorizing the scene, because the robot changes its location all the time, and the scene representation should be independent of the temporary point of observation. Thus, we have to transform the positions of the objects to some scene space.

3.1 Transforming camera into scene coordinates

In the real world there is no such thing, as global coordinates. Everything that we see, is seen from relative first-person perspective. But the memorized mental model of the world is a combination of numerous local scenes (episodes), which are combined into global memory, forming a hierarchical structure. The approach to structure the robot memory should be similar. In this paper we will focus on constructing memory within a single scene, and this approach can be extended to more scenes and complex worlds later.

If there are no global reference points, that means, that the coordinate system is arbitrary. The only requirement, is that it should be stable. But everything can move, so there are no fully reliable reference points. Our approach assumes, that every part of a scene can be a reference to the other parts of the same scene, or even other scenes. The location of an object within a scene can be determined, if

the robot perceives other, previously located reference objects within the same scene.
As demonstrated in Section 2, a single robot position allows for recording local object coordinates. Now it is time, to make the coordinates independent of the temporary position of the robot. Let us assume, the scene looks like in **Figure 7**. The triangle shows the depth camera view and range (dashed line). The image is only schematic, because there is no precisely defined range of the depth camera, as it depends on the surfaces visible in the scene. Within the camera view we have three visible objects: O1, O2, and O3. Thus **Figure 7** is the equivalent to the situation presented in **Figure 3**, where the robot can see three objects.

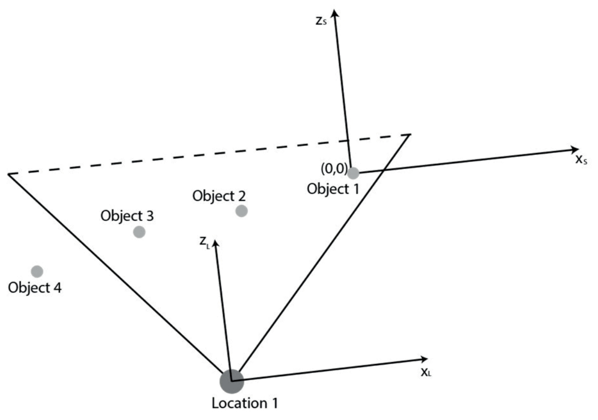

Figure 7 The sample scene seen from Location 1 (top view) – the first step of scene memory building

In the first step of its operation, the robot starts building its scene memory, which is based on the scene coordinate system. The scene coordinates have the same axes as camera, but the difference is that they are associated to the scene in a permanent way. The origin of the scene coordinates can be located in arbitrary point, like Object 1 in **Figure 7**. The scene coordinate axes (x_S,y_S,z_S) are parallel to the local camera view axes (x_L,y_L,z_L). Computing the scene coordinates of all visible objects is straightforward, given their local coordinates. It is enough to subtract from the scene coordinates of an object the camera coordinates of the origin of the scene coordinates

$$\begin{bmatrix} x \\ y \\ z \end{bmatrix}_{O_S} = \begin{bmatrix} x \\ y \\ z \end{bmatrix}_{O_{L1}} - \begin{bmatrix} x \\ y \\ z \end{bmatrix}_{(0,0,0)_{L1}} . \tag{1}$$

Also, the camera location in scene coordinates can be easily found by putting: $\begin{bmatrix} x \\ y \\ z \end{bmatrix}_{O_{L1}} = \begin{bmatrix} 0 \\ 0 \\ 0 \end{bmatrix}$

To simplify further considerations, and easily explain the idea of memory building, we have to take into account the technical limitations of the experiment. The main assumption is that the robot travels on a flat surface, and the camera is fixed to the robot, so the robot cannot change the angle of observation independently of its movement. This assumption leads to the situation, where the point of observation moves only in 2 dimensions, although the world it sees is 3D. We also assume that the y coordinate is constant, and movement of the robot can be expressed using only 2 Cartesian coordinates (x_S,z_S).
Let us now assume, that the robot moves from the original position L1 to a new location L2 (**Figure 8**). What has changed is that a new object appeared in robot's field of vision (Object 4). We know its local position obtained directly from the camera measurement. However, we do not know, how to determine its position with respect to the scene coordinates. Moreover, the scene origin in **Figure 8** is no longer visible. But this is not a problem as long, as the robot sees at least 2 objects, with known scene positions. In our case these are Object 2 and Object 3.

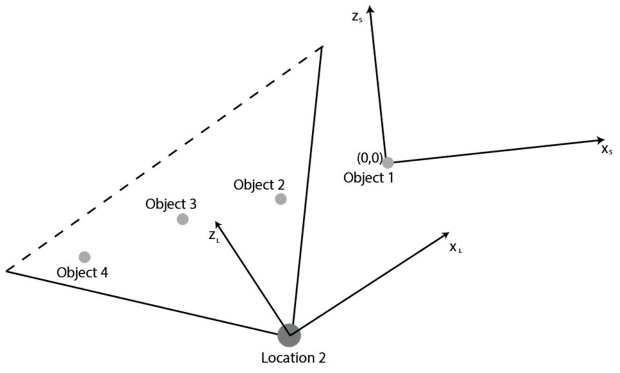

Figure 8 The view of the scene after robot moves to a new location

To determine the scene coordinates of a new object, we have to know, how the position of the robot has changed. We find that information by determining the relative robot motion with respect to the scene objects. To do that, it is convenient to describe the motion using polar coordinates, by combining robot motion from rotation, and translation. The scene coordinates of a new object are calculated by transforming the Location 2 coordinates into scene coordinates, as follows:

$$\begin{bmatrix} x \\ z \end{bmatrix}_S = R \begin{bmatrix} x \\ z \end{bmatrix}_{L2} + T - \begin{bmatrix} x \\ z \end{bmatrix}_{(0,0)_{L1}} , \tag{2}$$

where R , and T are the rotation translation matrices of the robot moving between L1 and L2. Explicitly this can be written as:

$$\begin{bmatrix} x \\ z \end{bmatrix}_S = \begin{bmatrix} r_{11} & r_{12} \\ r_{21} & r_{22} \end{bmatrix} \begin{bmatrix} x \\ z \end{bmatrix}_{L2} + \begin{bmatrix} t_x \\ t_z \end{bmatrix} - \begin{bmatrix} x \\ z \end{bmatrix}_{(0,0)_{L1}} \tag{3}$$

What we have to find, is the rotation, and translation parameters. To solve the problem, we move to the homogeneous coordinates, which leads to a single transformation matrix:

$$\begin{bmatrix} x \\ z \\ 1 \end{bmatrix}_S = T_R \begin{bmatrix} x \\ z \\ 1 \end{bmatrix}_{L2} , \tag{4}$$

or explicitly:

$$\begin{bmatrix} x \\ z \\ 1 \end{bmatrix}_S = \begin{bmatrix} cos\theta & -sin\theta & t_x - x_{(0,0)_{L1}} \\ sin\theta & cos\theta & t_z - z_{(0,0)_{L1}} \\ 0 & 0 & 1 \end{bmatrix} \begin{bmatrix} x \\ z \\ 1 \end{bmatrix}_{L2} , \tag{5}$$

where θ is the rotation angle of the local robot coordinates with respect to the scene coordinates. This is a single matrix equation, with 4 parameters to be determined. A single data point is insufficient to solve eq. (4), but when we combine equations for 2 points (objects *O2* and *O3* in **Figure 8**), the equation system becomes solvable:

$$\begin{cases} \begin{bmatrix} x \\ z \\ 1 \end{bmatrix}_{O2_S} = T_R \begin{bmatrix} x \\ z \\ 1 \end{bmatrix}_{O2_{L2}} \\ \begin{bmatrix} x \\ z \\ 1 \end{bmatrix}_{O3_S} = T_R \begin{bmatrix} x \\ z \\ 1 \end{bmatrix}_{O3_{L2}} \end{cases}, \quad (6)$$

To solve the system of equations let's express them in the following form (4 equations with 4 unknowns):

$$\begin{bmatrix} x_{O2_S} \\ z_{O2_S} \\ x_{O3_S} \\ z_{O3_S} \end{bmatrix} = \begin{bmatrix} cos\theta x_{O2_{L2}} - sin\theta z_{O2_{L2}} + t_x - x_{(0,0)_{L1}} \\ cos\theta z_{O2_{L2}} + sin\theta x_{O2_{L2}} + t_z - z_{(0,0)_{L1}} \\ cos\theta x_{O3_{L2}} - sin\theta z_{O3_{L2}} + t_x - x_{(0,0)_{L1}} \\ cos\theta z_{O3_{L2}} + sin\theta x_{O3_{L2}} + t_z - z_{(0,0)_{L1}} \end{bmatrix}, \quad (7)$$

or as a product:

$$\begin{bmatrix} x_{O2_S} \\ z_{O2_S} \\ x_{O3_S} \\ z_{O3_S} \end{bmatrix} = \begin{bmatrix} x_{O2_{L2}} & -z_{O2_{L2}} & 1 & 0 \\ z_{O2_{L2}} & x_{O2_{L2}} & 0 & 1 \\ x_{O3_{L2}} & -z_{O3_{L2}} & 1 & 0 \\ z_{O3_{L2}} & x_{O3_{L2}} & 0 & 1 \end{bmatrix} \begin{bmatrix} cos\theta \\ sin\theta \\ t_x - x_{(0,0)_{L1}} \\ t_z - z_{(0,0)_{L1}} \end{bmatrix}, \quad (8)$$

where $\begin{bmatrix} x_{O2_S} \\ z_{O2_S} \\ x_{O3_S} \\ z_{O3_S} \end{bmatrix}$ are known coordinates, because we determined them in the previous iteration, and $\begin{bmatrix} x_{O2_{L2}} \\ z_{O2_{L2}} \\ x_{O3_{L2}} \\ z_{O3_{L2}} \end{bmatrix}$ are also known because they are determined locally. To get the desired parameters $\begin{bmatrix} cos\theta \\ sin\theta \\ t_x - x_{(0,0)_{L1}} \\ t_z - z_{(0,0)_{L1}} \end{bmatrix}$, it is enough to find the inverse of the transformation matrix, and multiply it by the vector of known scene coordinates:

$$\begin{bmatrix} cos\theta \\ sin\theta \\ t_x - x_{(0,0)_{L1}} \\ t_z - z_{(0,0)_{L1}} \end{bmatrix} = \begin{bmatrix} x_{O2_{L2}} & -z_{O2_{L2}} & 1 & 0 \\ z_{O2_{L2}} & x_{O2_{L2}} & 0 & 1 \\ x_{O3_{L2}} & -z_{O3_{L2}} & 1 & 0 \\ z_{O3_{L2}} & x_{O3_{L2}} & 0 & 1 \end{bmatrix}^{-1} \begin{bmatrix} x_{O2_S} \\ z_{O2_S} \\ x_{O3_S} \\ z_{O3_S} \end{bmatrix}, (9)$$

The inverse of the transformation matrix can be found algebraically or numerically. In our experiments we use the numerical solution. Given the transformation parameters, we can compute scene coordinates of all the newly seen objects using eq. (5), which transforms the local coordinates of objects to their scene coordinates.

The two objects in the scene coordinates are the minimal number of objects that must be used to determine the robot transformation parameters. In case of more objects, previously located in the scene coordinates and present in the field of view, all of them can be used to increase reliability of the computation and reduce the solution error that may result from imperfect measurements. We can take pairs of such objects, determine the transformation parameters from each of the pairs, and average the results or combine all previously located object coordinates to obtain one overdetermined system of equations. Solution of such system yields the smallest least square error for given set of measurements.

The limitation of the method, to some degree, is the requirement, that the robot needs to have at least two objects within the field of view, to be able to determine its own transition within the scene, as well as locations of new objects. To satisfy this requirement, the masking algorithm should be trained to recognize as many object types as possible. But still there is a chance that the robot, can stand in front of a wall, and lose any recognizable objects from its view. In this situation, the robot should start exploring the scene in a random way, to find any recognizable object. Then there are two possible cases. The first one is that the scene the robot sees, is already memorized one. In this case the robot is able to recognize its location within the scene, and continue the exploration of the known environment. The other case is the situation, where the robot does not recognize the visible combination of objects. In this case, it should build the new scene memory. It is possible, that it will find the relation between the two scenes later. Similar situation is when the robot is switched off to break the experiment, moved to some other location, and then switched on again to start the experiment. The robot's memory is maintained, because it is kept on the server, and the robot only connects to the memory when it is running. In consequence of such approach, the robot spatial memory consists of a number of smaller scenes. The relation between different parts of memory can be found at later time, when the robot finds object combination on the boundary of two scenes. Actually, in such cases, the coordinates of objects in one scene could be recalculated to make all objects match the common coordinate system. This makes sense if there are many points shared between the scenes, like objects in the same room. In case of very few contact points (like in case of separate rooms), it is more convenient to leave both scenes separate and only memorize the relationship between scenes. The detailed discussion of this issue goes beyond the scope of this article, and will be discussed separately.

3.2 Experimental results

Now we will illustrate the presented considerations with the results of an experiment. In **Figure 3** we presented the initial scene view with masked objects. The respective top view of the point cloud, filtered using the masks, is presented in **Figure 9**. In this iteration the robot locates the scene coordinate origin in arbitrary object. In our case this is a gray chair visible to the right (O1). The axes of the scene coordinate system are parallel to the local camera coordinates.

The robot starts traveling across the scene. Its motion is a combination of rotation and translation. The next view that the robot registered is shown in **Figure 10**. What has changed within the scene view is that a new object was identified (orange pouf), and one of the previously seen gray chairs is no longer within the field of view. This kind of scene view change was illustrated in **Figures 7** and **8**.

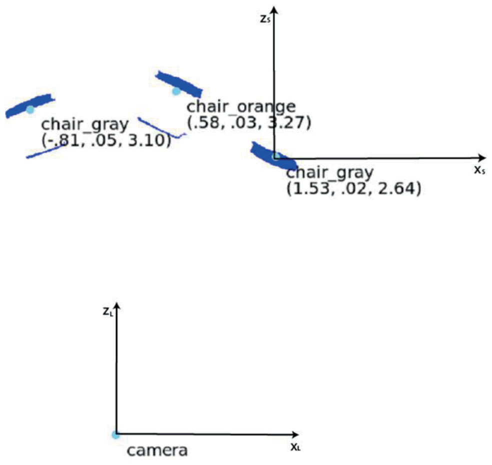

Figure 9 The top view of the point cloud – initial robot location

Let us see the top view of the point cloud of the second view (**Figure 11**). The goal of the robot is to locate the orange pouf within the scene coordinates. The scene coordinate origin is no longer visible, but it is enough that the scene position of gray chair and orange chair are already known.

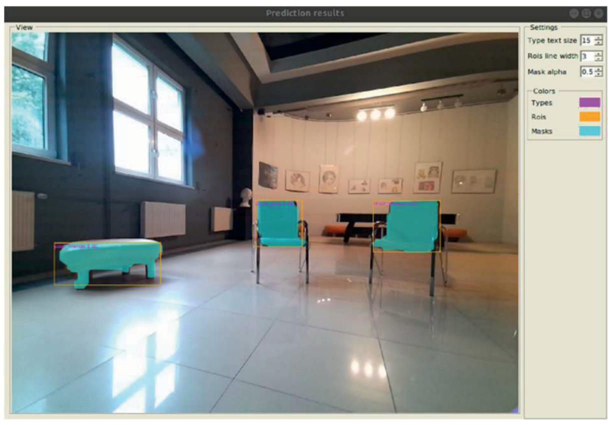

Type text size 15
Rois line width 3
Mask alpha 0.5
Types 🟪
Rois 🟧
Masks 🟦

Figure 10 The second scene view with masked objects

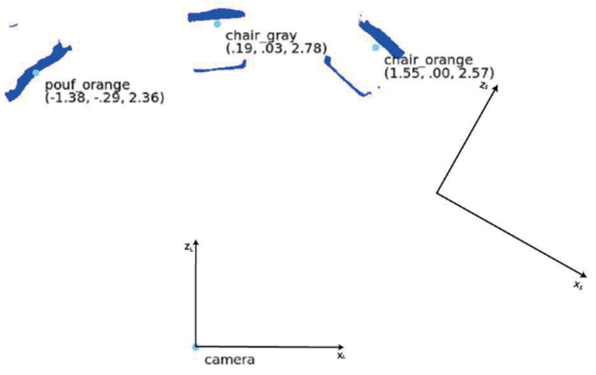

Figure 11 The second scene top view with masked objects

Let us have a closer look at the calculations performed during the presented experiment. In Location 1 (**Figure 7**), the coordinates of objects of interest are the following:
$O1_{L1} = [1.53, 0.02,\ 2.64]$,
$O2_{L1} = [0.58, 0.03, 3.27]$,
$O3_{L1} = [-0.81, 0.05, 3.10]$.
These are the camera coordinates expressed in meters. Making them scene coordinates is easy, because it requires subtracting the coordinates of object that serves as the origin of the scene coordinates. In our case this is the $O1$ object. In this way we get scene coordinates of objects:
$O1_S = [0.0,\ 0.0, 0.0]$,
$O2_S = [-0.95, 0.01, 0.63]$,
$O3_S = [-2.34, 0.03, 0.46]$.
Then the robot moves to Location 2, and our goal is to determine the scene coordinates of object 4. For this purpose we need the camera coordinates of objects 2 and 3 in L2:
$O2_{L1} = [1.55, 0.00, 2.57]$,
$O3_{L1} = [0.19, 0.03, 2.78]$.
Next we find the solution of Equation 9, which yields the vector specifying the transformation parameters:

$$\begin{bmatrix} cos\theta \\ sin\theta \\ t_x \\ t_z \end{bmatrix} = \begin{bmatrix} 0.98 \\ 0.28 \\ -0.23 \\ 0.32 \end{bmatrix}, \qquad (10)$$

From the above we can find the rotation angle of the robot between L1 and L2, which is 12°. The camera coordinates of Object 4 recorded in L2 are: $O4_{L2} = [-1.38, -0.29, 2.36]$. After applying equation 5, with parameters 10, we get the following scene coordinates: $O4_S = [-3.76, -0.41, -0.39]$.

3.3 The system efficiency

The computer that runs all the processing of data delivered by the robot is equipped with two Intel Xeon CPU E5-2697, which allow for running up to 72 processes simultaneously. It is also equipped with 3 GPU cards: NVIDIA RTX 2080ti, TITAN Xp, and TITAN X. The most important factor influencing the speed of processing is the possibility of accelerating the computational tasks on the GPU-s. The element that consumes most of the computational power is the YOLACT masking algorithm. The time of processing a single frame from the camera on the RTX device takes about 33ms. The other elements of the computational chain were also implemented using CUDA to use the GPU acceleration. The most important tasks are: transforming depth data into point cloud, filtering the cloud with the masks, and computing object locations. Actually, we are using 2 GPU-s. While on one GPU the operations related to the point cloud processing are performed, the other GPU computes the masks for the next frame. Sequential processing of these two tasks on a single GPU would cause additional delay. The multiple CPU power is used only in a minor way.
In consequence of the presented approach to computations, we are able to process each scene about 15 times per second, which includes the masking, and the depth data processing. For the purpose of the experiment, this is very fast.

4 Conclusions

We demonstrated a method for building spatial scene memory. The advantage of this method is minimal requirement with respect to the storage, because the objects are represented as single points. This kind of representation should allow for quick real time searching and comparison of different scenes, even if the scenes are large and complex. In this way, the robot is able to find the relation between what is sees, and what is memorized, using the distance matrix method. The whole robot memory is built as a collection of different scenes, which can be combined, when the robot finds relation between them. The details of how the system compares, and recognizes scenes will be demonstrated in a separate paper.
The presented solution was demonstrated for a limited case of a robot moving on a flat surface, which results in a constant height, and simplifies the computations. The solution however can be extended to arbitrary kind of motion in 3D. The only difference in case of a robot moving freely in 3D is that it has to follow at least 3 objects to be able to assess its own motion (our simplified 2D case requires only 2 objects).
The hardware solution and the code that we developed, heavily relies on using GPU for acceleration. This allowed us to achieve high processing speed, which is sufficient for performing experiments with the current solution, and further extending the functionalities of the robot.
The method relies on an external tool, which is the instance segmentation algorithm. Despite huge progress in this field, such algorithms have their limitations, which were partially discussed in the paper. Considering the effort taken to improve this kind of tools all around the world, the situation should improve in the future.
The demonstrated perception and memory system could serve many various purposes. It could be used in an inspection robot, which monitors locations of various kinds of objects, like goods in a warehouse, or cars in a parking lot. In our research we plan to use the robot to implement a Motivated Learning scenario [16], where the robot will be able to find and memorize objects in its environment, and satisfy its needs by performing suitable operations on the objects.

Acknowledgement

This work was supported by the grant from the National Science Centre DEC-2016/21/B/ST7/02220.

5 Literature

[1] Cadena, C.: Carlone, L.: Carrillo, H: Latif, Y.: Scaramuzza, D.: Neira, J.: Reid, I.: Leonard, J.J.: Past, Present, and Future of Simultaneous Localization and Mapping: Toward the Robust-Perception Age. IEEE Transactions on Robotics. 32 (6): 2016, pp. 1309–1332

[2] Karlsson, N.: Di Bernardo, E.: Ostrowski, J.: Goncalves, L.: Pirjanian, P.: Munich, M.: The vSLAM Algorithm for Robust Localization and Mapping. Int. Conf. on Robotics and Automation, ICRA, 2005

[3] Newcombe, R.A.: Izadi, S.: Hilliges, O.: Molyneaux, D.: Kim, D.: Davison, A.J.: Kohi, P.: Shotton, J.: Hodges, S.: Fitzgibbon, A.: KinectFusion: Real-time dense surface mapping and tracking. In Proceedings of the 2011 10th IEEE International Symposium on Mixed and Augmented Reality, Basel, Switzerland, 26–29 October 2011, pp. 127–136

[4] Endres, F.: Hess, J.: Sturm, J.: Cremers, D.: Burgard, W.: 3-D mapping with an RGB-D camera. Transactions on Robotics 30, 2014, pp. 177–187.

[5] Hosseinzadeh, M.: Latif, Y.: Pham, T.: Suenderhauf, N.: Reid, I.: Towards Semantic SLAM: Points, Planes and Objects, 2018 arXiv:1804.09111v1

[6] Kaneko, M.: Iwami, K.: Ogawa, T.: Yamasaki, T.: A-izawa, K.: Mask-SLAM: Robust feature-based monocular SLAM by masking using semantic segmentation, IEEE/CVF Conference on Computer Vision and Pattern Recognition Workshops (CVPRW), Salt Lake City, UT, 2018, pp. 371-3718

[7] Guan, P.: Cao1, Z.: Chen, E.: Liang, S.: Tan, M.: Yu, J.: A real-time semantic visual SLAM approach with points and objects, International Journal of Advanced Robotic Systems, vol. 17, no. 1, 2020

[8] Goodfellow, I.: Bengio Y.: Courville A.: Deep Learning, MIT Press, 2016 http://www.deeplearningbook.org

[9] Ren, S.: He, K.: Girshick, R.: Sun, J.: Faster R-CNN: Towards Real-Time Object Detection with Region Proposal Networks, 2016 https://arxiv.org/abs/1506.01497

[10] He, K.: Gkioxari, G.: Dollár, P.: Girshick, R.: Mask R-CNN, 2017 https://arxiv.org/abs/1703.06870

[11] Redmon, J., Divvala, S.: Girshick, R. Farhadi, A.: You Only Look Once: Unified, Real-Time Object Detection, 2015 https://arxiv.org/abs/1506.02640

[12] Bolya, D.: Zhou, C.: Xiao, F.: Lee, Y.J.: YOLACT: Real-time Instance Segmentation, ICCV, 2019

[13] Trevor, A.J.B.: Rogers, J.G.: Christensen, H. I. Planar Surface SLAM with 3D and 2D Sensors. In IEEE International Conference On Robotics and Automation, St. Paul, MN, 2012

[14] Kim, B.: Kohli, P.: Savarese, S.: 3D Scene Understanding by Voxel-CRF, The IEEE International Conference on Computer Vision (ICCV), 2013, pp. 1425-1432

[15] Jaszuk, M.: Starzyk, J.A.: Building Internal Scene Representation in Cognitive Agents, Knowledge, Information and Creativity Support Systems: Recent Trends, Advances and Solutions, Andrzej M.J. Skulimowski, Janusz Kacprzyk eds, in series: Advances in Intelligent Systems and Computing, 364, Springer, 2016, pp. 479-491

[16] Starzyk, J.A.: Graham. J.: MLECOG - Motivated Learning Embodied Cognitive Architecture, IEEE Systems Journal, vol. 11, no. 3, 2017, pp. 1272-1283